RSC Advances

ROYAL SOCIETY OF CHEMISTRY

www.rsc.org/advances

For Table of Contents Use Only

One-Step Synthesis of Urchin-Like Sulfur/Polyaniline Nano-Composite as Promising Cathode Material for High-Capacity Rechargeable Lithium-Sulfur Battery

Qi Lu,[a,¶] Hong Gao,[a,b,¶] Yujie Yao, Nianjiang Liu,[a] Xianhong Wang,*[,a] and Fosong Wang[a]

[a] Key Laboratory of Polymer Eco-materials, Changchun Institute of Applied Chemistry, Chinese Academy of Sciences, Changchun 130022, People's Republic of China

[b] University of Chinese Academy of Sciences, Beijing 100039, People's Republic of China

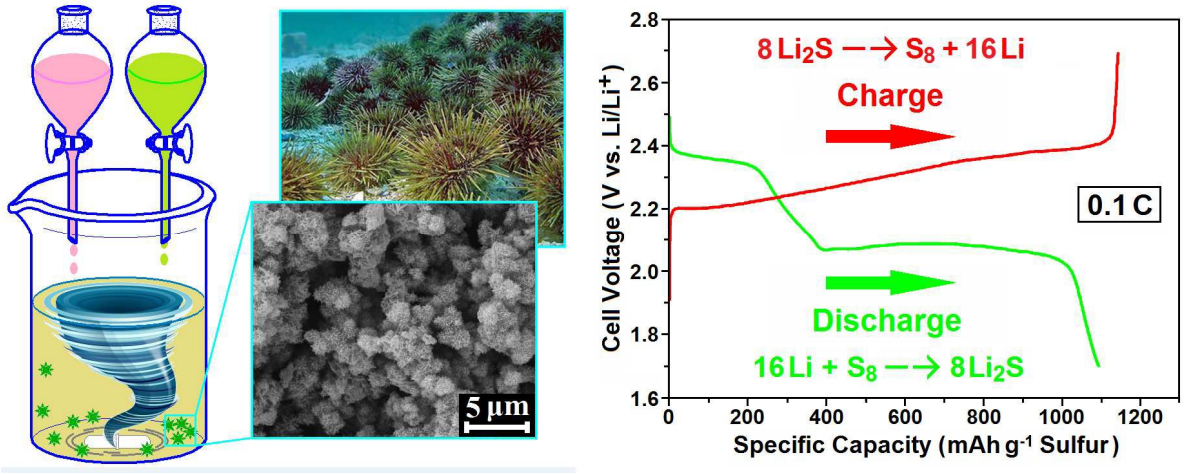

Cite this: DOI: 10.1039/c0xx00000x

www.rsc.org/xxxxxx

COMMUNICATION

One-Step Synthesis of Urchin-Like Sulfur/Polyaniline Nano-Composite as Promising Cathode Material for High-Capacity Rechargeable Lithium-Sulfur Battery

Qi Lu,[a,¶] Hong Gao,[a,b,¶] Yujie Yao,[a,b] Nianjiang Liu,[a] Xianhong Wang*[a] and Fosong Wang[a]

Received (in XXX, XXX) Xth XXXXXXXXX 20XX, Accepted Xth XXXXXXXXX 20XX
DOI: 10.1039/b000000x

Urchine-like sulfur/polyaniline (S/PANI) nano-composite has been synthesized by a very soft and facile approach. This novel composite could be directly utilized as the cathode material for lithium-sulfur (Li-S) battery and display high specific capacity at different discharge current densities and good stability over long-term cycling.

Recently, clean and renewable energy sources like solar, wind, and tidal energy, etc., have received increasing attention.[1-3] As one of the most important components for clean energy system, energy storage devices with much higher energy density, excellent rate performance and long-life cycling stability are badly needed than at any time in the past.[4,5] Unlike traditional intercalation mechanism utilized in current lithium-ion battery (LIB), lithium-sulfur (Li-S) battery depends on a two-electron reaction, $16Li + S_8 \rightarrow 8Li_2S$, and has a fabulous theoretical energy density of 2567 Wh kg^{-1} making it a very promising candidate for next generation energy storage device.[6-8] In addition to its high theoretical energy density, compared with common transition metal oxide compounds, choosing S as the battery active substance has extra bonus like natural abundance, low cost, and non-toxicity, etc.[9] However, there are still two major challenges need to be dealt with at present, one is the extremely low electrical conductivity of elemental S which leads to low utilization of the active material and bad rate performance of the battery. The other is the high solubility of the polysulfide intermediate formed during the charging-discharging cycles, which could seriously destroy the cycling stability of the battery by a so-called "shuttle phenomenon".[10-12] To overcome the two problems, much effort has been devoted to designing and preparing novel composite cathode materials, based on S and various kinds of carbon, for instance, carbon micro-sphere,[13] carbon nanotube/nanofiber,[14-16] meso-porous carbon,[17,18] and graphene.[19-22] In these composites, the carbon serves as a high performance electron conducting matrix, and at the same time, its special micro- or nano-structure could provide a physically trapping effect to the polysulfide. Although this strategy achieved an obvious improvement for the Li-S battery, the diffusion and aggregation of S exist over long-term cycling.[5,10] Recently, conducting polymers were introduced into this research field due to their adjustable morphology, favorable redox activity, and especially, strong electrostatic interaction with the polysulfide.[23-25] Liu and colleagues prepared a novel S/PANI nano-fibers with good cycling performance by heating the mixture of S and PANI at 280 ℃.[26] Chen et al. explored a relatively simple one-step method to prepare the sulfur/polypyrrole (S/PPY) composite at room temperature, however, its capacity reduced 60% after only 40 cycles.[27] Manthiram and Fu synthesized two types of S/PPY composites and carefully investigated their short-term cycling stability.[28,29] Abruña and co-workers reported a particular S/PANI yolk-shell composite with a stable capacity of 765 mAh g^{-1} S at 0.2 C after 200 cycles.[30] Cui et al. systematically compared the influence of PNAI, PPY and poly(3,4-ethylenedioxythiophene) (PEDOT) on the performance of S-conducting polymer composite cathodes.[31] All of these research work intensively demonstrated the potential of conducting polymers, while developing new kinds of composite cathode materials with better performance by more simple approach would be the future research focus.

Herein, we synthesized a novel S/PANI nano-composite with three-dimensional urchin-like structure and 55% sulfur content by a very soft and facile one-step approach, and then, systematically investigated its properties and potential application for the rechargeable Li-S battery. It was found that this novel composite could (1) be directly utilized as the cathode material without any conducting additive, (2) achieve an initial discharge capacity of 1095 mAh g^{-1} at 0.1 C, nearly 66% of the theoretical value and five times higher than that of current commercial LIB, and (3) retain a discharge capacity of more than 832 mAh g^{-1} at 0.2 C and 609 mAh g^{-1} at 1.0 C, and meanwhile, a relatively high Coulombic efficiency of nearly 96% over 100 cycles.

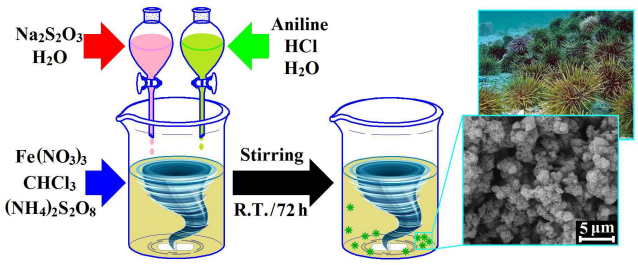

Fig. 1 Scheme of the urchin-like S/PANI nano-composite preparation.

The S/PANI nano-composite was prepared by a synthetic approach outlined in Figure 1. First, sodium hyposulfite ($Na_2S_2O_3$) and aniline monomer were dissolved in de-ionized

water and dilute hydrochloric acid to form two homogeneous solutions. Then, they were dropped into the solution of ferric nitrite ($Fe(NO_3)_3$) and ammonium persulphate ($(NH_4)_2S_2O_8$) in chloroform ($CHCl_3$) slowly at room temperature. Two reactions occurred simultaneously in the system:

(1) Heterogeneous sulfur nucleation reaction:

$$Na_2S_2O_3 + 2HCl \rightarrow S\downarrow + H_2O + 2NaCl + SO_2\uparrow,$$

(2) Aniline polymerization initiated by Fe^{3+} and $S_2O_8^{2-}$.

By adjusting the reaction conditions, such as time, temperature, or reagents ratio, it was possible to form distinctive S/PANI composite with special morphology and component (more synthesis data has been given in Supporting Information). After a violent stirring for 72 hours at room temperature, the mixture was filtered and washed by large amounts of ethanol and de-ionized water for three times to remove the survival reactants. Finally, the light green mass was dried at 60℃ for 24 hours under vacuum to give the pure S/PANI powder.

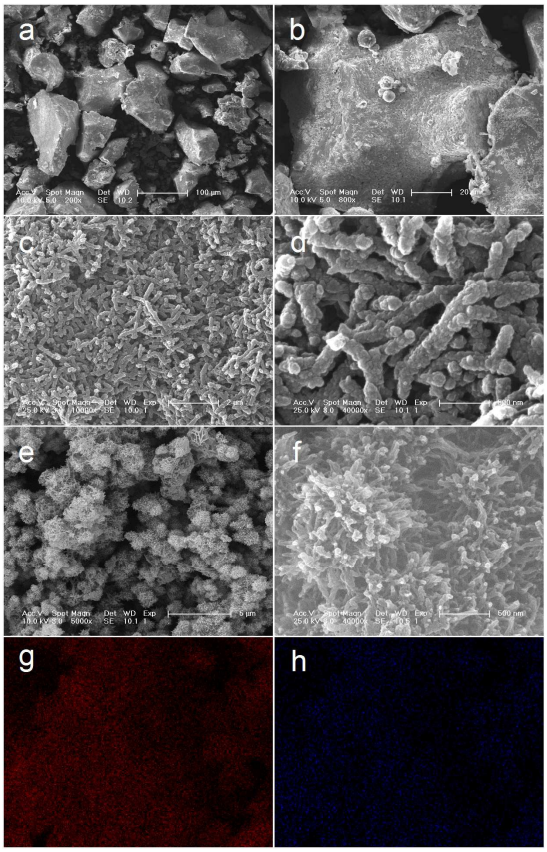

Fig. 2 SEM images of the deposition pure S (a, b), PANI nano-rods (c, d), S/PANI nano-composite with different magnification (the scale bar in Figure 2e is 5 μm, while it is 500 nm in Figure 2f) and the corresponding elemental mappings of C and S (g, h).

The morphology and composition of this S/PANI nano-composite were studied by the scanning electron microscopy (SEM) observation. For a comparison, the SEM images of deposition pure S and PANI nano-rods synthesized by the similar method were illustrated in Figure 2a-2d (synthesis detail has been given in Supporting Information). It is clear that the pure deposition S had typical massive shape with characteristic dimensions in dozens of micrometers, while the PANI nano-rods had far smaller size with diameter of approximate 130 nm and length of about 460 nm, meanwhile, with the Brunauer-Emmett-Teller (BET) surface area of about 35.8 m^2/g (see Figure S2a). However, as shown in Figure 2e, the S/PANI composite showed an obvious three-dimensional urchin-like structure, the typical dimension of single microsphere was *Ca.* 890 nm in diameter. For more detailed analysis, a zoom-in SEM image was captured (see Figure 2f), which illustrated clearly that each microsphere was composed by hundreds of radiate nano-fibers with diameter of approximate 38 nm and length of about 220 nm. This specific nano-structure with the larger BET surface area of approximately 122.6 m^2/g (see Figure S1b) was similar to the conducting polymer parallel array utilized in the research field of super-capacitor, that could enlarge the contact area between the active substance and electrolyte, and increase the total ion conductivity substantially.[32] Figure 2g and 2h displayed the corresponding elemental maps of C and S obtaining by the energy-dispersive spectroscopy (EDS), and the C and S signals were detected uniformly over the whole field of vision, indicating the S was fully distributed with the PANI in this composite.

Figure 3a showed the FT-IR spectra of PANI nano-fibers (PANI-NF, prepared as our previous report)[33] and S/PANI nano-composite. For PANI-NF, the peaks at 1582 cm^{-1} and 1462 cm^{-1} were consistent with C=C stretching de-formation of quinoid and benzene rings, respectively. The bands at 1298 cm^{-1} and 1131 cm^{-1} could be attributed to C-N stretching of secondary aromatic amine and the aromatic C-H in-plane bending. The peaks at 790 cm^{-1} and 504 cm^{-1} could be attributed to the out-of-plane deformation of C-H in the 1,4-dissubstituted benzene ring. For S/PANI composite, the absorption peaks were almost identical to that of PANI-NF, and the changes at 675 cm^{-1}, 1270 cm^{-1}, 2835 cm^{-1} and 2925 cm^{-1} were consistent with the previous report about the IR absorption of the elemental sulfur, indicating that the chemical structures of PANI in both of them were basically similar.[34]

Figure 3b showed the X-ray diffraction (XRD) data of S, PANI-NF and S/PANI nano-composite. The positions and intensities of the reflections of the S showed an evident characteristic of Fddd orthorhombic structure. While the XRD data of PANI-NF showed a typical amorphous characteristic with two broad peaks centered at $2\theta = 19^\circ$ and 25.6°, which could be assigned as the periodicity parallel and perpendicular to the PANI chains, respectively. The XRD data of S/PANI composite was almost a linear superposition of them demonstrating that the S formed by heterogeneous nucleation retained its original crystal structure even after aniline polymerization on its surface.

To confirm the valence of S atom in the S/PANI nano-composite, the X-ray photoelectron spectroscopy (XPS) spectra of the S 2p for $Na_2S_2O_3$, S/PANI composite and elemental S were illustrated in Figure 3c. Two types of S atoms in $Na_2S_2O_3$ were observed with the binding energies of 162.3 eV and 168.4 eV. The peak at 168.4 eV was assigned to the S atom connected with three O atoms by double bond, and the peak at 162.3 eV was assigned to the S atom connected with the former S atom by a single bond. For the S/PANI composite, two peaks with much less energy separation were observed in the fitted curves (dashed lines) with the binding energies of 163.5 eV and 164.3 eV. By compared with the XPS spectrum of S, the two peaks respectively corresponded to the S $2p_{3/2}$ and S $2p_{1/2}$ components, indicating the

formation of elemental S in the S/PANI composite.

The thermogravimetric analysis (TGA) was performed to determine the mass percentage of S in the S/PANI nano-composite. As shown in Figure 3d, the elemental S started a weight loss at 120℃ and lost its all weight at 300℃. The PANI-NF exhibited two stages of weight loss, the first one started at 35 ℃, which was due to the loss of moisture, and the second one started at 179℃, which was due to the decomposition of PANI itself. It was very easy to conclude that this S/PANI composite was composed of 55% S and 45% PANI.

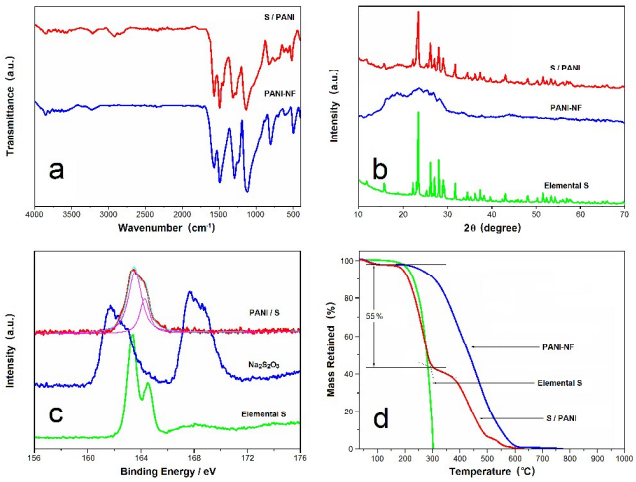

Fig. 3 FT-IR spectra of S/PANI composite and pure PANI (a), XRD spectra of the S/PANI composite and pure PANI, and elemental S (b), XPS spectra of S 2p for S/PANI composite, $Na_2S_2O_3$ and elemental S (c), and TGA curves of S/PANI composite and $Na_2S_2O_3$ (d).

To fabricate a composite cathode for Li-S battery, 180 mg S/PANI composite, 20 mg cation aqueous polyurethane resin adhesive and 2 g de-ionized water were mixed to make a relatively homogeneous mixture at room temperature. It was then coated on an aluminum foil and dried at 60℃ for 36 hours in vacuum oven. The 2032-type coin cell was used for the electrochemical test with thin lithium foil as the anode. The electrolyte was lithium bis(trifluoromethanesulfonyl) imide (LiTFSI) and $LiNO_3$ in the mixture of 1,2-dimethoxyethane and 1,3-dioxolane (1:1, v/v). The typical mass loading of cathode material was 2.0 mg/cm^2. A glass microfiber filter paper was used as separator, its high intensity could avoid the short circuit caused by the formation of lithium dendrite during the charge process.

The cyclic voltammertric (CV) curves of the electrode made by the S/PANI nano-composite were shown in Figure 4a. The two reduction peaks at 2.31 V and 2.01 V corresponded to the conversion process of high-ordered polysulfide to low-ordered polysulfide, and then, to Li_2S solid. The single oxidation peak at 2.58 V should be an overlap of two peaks corresponded to the reversible process of Li_2S to high-ordered polysulfide. The approximately equal intensities of the reduction and oxidation currents revealed a high Coulomic efficiency. When the cycling number increased, the redox current intensity and peak positions exhibited very slight changes, indicating that this S/PANI composite had excellent electrochemical stability in the voltage range between 1.5 V and 3.0 V (vs Li/Li$^+$).

Figure 4b showed the charge-discharge curves of the Li-S battery based on the S/PANI composite cathode at 0.1C rate. The two voltage plateaus during the discharge processes corresponded with the two reduction peaks in Figure 4a, and the same as the CV test, both of them remained constant over a long-term cycling. The initial discharge specific capacity of this S/PANI composite achieved 1095 mAh g^{-1}, which was nearly five times higher than that of current commercial LIB, however, considering only 66% S in the S/PANI composite was utilized, there was still huge rise space for this material. After 50 cycles, the discharge specific capacity reduced 12% to 964 mAh g^{-1}, and meanwhile, the Coulomic efficiency also decreased to some degree.

The rate capability of this S/PANI composite was evaluated by a cycling test carried out at different current densities from 0.1 C to 1.0 C, and then back to 0.1 C. As illustrated in Figure 4c, the discharge specific capacity of the S/PANI composite decreased from 1098 mAh g^{-1} at 0.1 C to 933, 827, and 682 mAh g^{-1} at 0.2 C, 0.5 C, and 1.0 C, respectively, and at high current density, the reduction of discharge specific capacity was less than 3% after 10 cycles, indicating that the nano-structure of S/PANI composite kept stable even under that condition. When the current density switched back to 0.1 C, the discharge specific capacities at each rate all showed obvious reversibility compared with the corresponding cycles, indicating that this S/PANI composite possessed good rate performance.

For S-conducting polymer composite, its relatively bad cycling stability in Li-S battery was a long-term unsolved major disadvantage. Here, we evaluated the cycling performance of this S/PANI composite at two different rates, as shown in Figure 4d. At 0.2 C, the initial discharge specific capacity of 978 mAh g^{-1} was achieved, and after 100 cycles, the capacity reduced 15% to 832 mAh g^{-1}. And at 1.0 C, this composite exhibited a better cycling performance with 12% capacity degradation from 689 to 609 mAh g^{-1}, which was mainly due to the attenuation of "shuttle phenomenon" under the larger current density.[10] Although there was still an obvious gap between this composite and the thermal treated (usually ＞ 250 ℃) S/C materials, that was an improvement for the S-conducting polymer composite, especially the S/PANI system prepared by a very facile one-step approach. Moreover, this composite retained a high Coulombic efficiency of nearly 96% over the 100 cycles, which again demonstrated its potential application in the rechargeable Li-S battery.

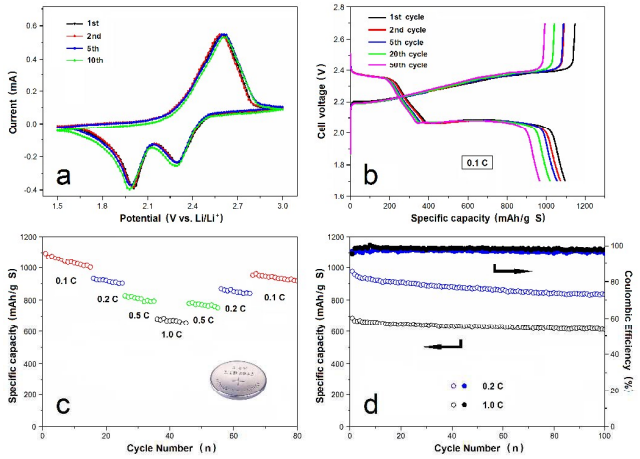

Fig. 4 The cyclic voltammograms of the S/PANI composite electrode (a), the discharge-charge curves of the Li-S battery based on S/PANI cathode (b), the rate performance (c) and cycling performance tests (d) of this Li-S battery.

To obtain a further insight into the interfacial charge transport and Li ion diffusion processes in this S/PANI nano-composite, electrochemical impedance spectroscopy (EIS) measurements were utilized on a S/PANI composite electrode. As showed in Figure 5, the EIS spectra of the S/PANI electrode at the 1st, 5th and 30th cycles all comprised a depressed semicircle at the high-frequency region and an inclined tail in the low-frequency region. The intercept at the real axis Z' of the EIS spectra corresponded to the combined resistance R_e, which was closely related to the resistance of S/PANI composite, the ionic resistance of the electrolyte, and the contact resistance at the interface between S/PANI composite and current collector. The R_e for the first cycle was 11.3 Ω and increased to 12.8 Ω after cycling for 5 cycles, then to 14.9 Ω after 30 cycles. The semicircle in the high-frequency region was related to the interface charge transport process of the S/PANI composite cathode, and the diameter of this semicircle corresponded to the charge transport resistance R_{ct}. The R_{ct} simulated from the equivalent circuit (inset in Figure 5) were 388.4, 417.8 and 442.3 Ω after the 1st, 5th and 30th cycles, respectively. The small increases of both R_e and R_{ct} over 30 cycles indicated that the interfacial charge transport and Li ion diffusion processes were not seriously influenced by the cycling number, namely, the morphological characteristics of S/PANI composite were preserved firmly during the long-term cycling.

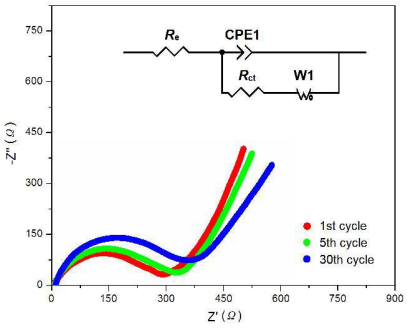

Fig. 5 The EIS spectra of the fresh prepared S/PANI composite electrode at different cycle numbers, and inset is the simulative equivalent circuit.

In summary, the novel urchin-like S/PANI nano-composite had been synthesized by a very facile and soft one-step approach and employed in rechargeable Li-S battery for the first time. The experimental result demonstrated that this low cost and easily produced composite could be directly utilized as the cathode material without any conducting additive. Its specific three-dimensional structure could enlarge the contact area between the active substance and electrolyte, and increase the total ion conductivity substantially. At 0.1 C, this composite displayed an initial discharge capacity of 1095 mAh g^{-1}, nearly 66% of the theoretical value and five times higher than that of current commercial LIB. Over 100 cycles, this composite still retained a discharge capacity of more than 832 mAh g^{-1} at 0.2 C and 609 mAh g^{-1} at 1.0 C, and meanwhile, a high Coulombic efficiency of nearly 96%. Additional EIS measurements provided a further insight into the interfacial charge transport and Li ion diffusion processes in this composite. More importantly, this research may give a new choice for fabrication of high-capacity rechargeable Li-S battery for practical application.

The authors thank financial support from the Natural Science Foundation of China (Grant Nos. 51321062 and 51303168).

Notes and references

[a] *Key Laboratory of Polymer Eco-materials, Changchun Institute of Applied Chemistry, Chinese Academy of Sciences, Changchun 130022, People's Republic of China. Fax: 86 431 85689095; Tel: 86 431 85262250; E-mail: xhwang@ciac.jl.cn*

[b] *University of Chinese Academy of Sciences, Beijing 100039, People's Republic of China.*

¶ *The authors contributed to this study equally.*

† Electronic Supplementary Information (ESI) available: Experimental details and additional data. See DOI: 10.1039/b000000x/

1 L. Nyholm, G. Nyström, A. Mihranyan and M. Strømme, *Adv. Mater.*, 2011, **23**, 3751-3769.
2 C. Liu, F. Li, L. P. Ma and H. M. Cheng, *Adv. Mater.*, 2010, **22**, E28-E62.
3 F. Cheng, J. Liang, Z. Tao and J. Chen, *Adv. Mater.*, 2011, **23**, 1695-1715.
4 P.G. Bruce, S. A. Freunberger, L. J. Hardwick and J. M. Tarascon, *Nat. Mater.*, 2012, **11**, 19-29.
5 A. Manthiram, Y. Fu and Y. S. Su, *Acc. Chem. Res.*, 2013, **46**, 1125-1134.
6 X. Ji and L. F. Nazar, *J. Mater. Chem.*, 2010, **20**, 9821-9826.
7 S. Evers and L. F. Nazar, *Acc. Chem. Res.*, 2013, **46**, 1135-1143.
8 D. W. Wang, Q. Zeng, G. Zhou, L. Yin, F. Li, H. M. Cheng, I. R. Gentle and G. Q. M. Lu, *J. Mater. Chem. A*, 2013, **1**, 9382-9394.
9 J. Q. Huang, X. F. Liu, Q. Zhang, C. M. Chen, M. Q. Zhao, S. M. Zhang, W. Zhu, W. Z. Qian and F. Wei, *Nano Energy*, 2013, **2**, 314-321.
10 A. Manthiram, Y. Fu, S. H. Chung, C. Zu and Y. S. Su, *Chem. Rev.*, 2014, **114**, 11751-11787.
11 N. Brun, K. Sakaushi, L. Yu, L. Giebeler, J. Eckert and M. M. Titirici, *Phys. Chem. Chem. Phys.*, 2013, **15**, 6080-6087.
12 S. H. Chung and A. Manthiram, *J. Mater. Chem. A*, 2013, **1**, 9590-9596.
13 W. Weng, V. G. Pol and K. Amine, *Adv. Mater.* 2013, **25**, 1608-1615.
14 J. Guo, Y. Xu and C. Wang, *Nano Lett.*, 2011, **11**, 4288-4294.
15 L. Ji, M. Rao, S. Aloni, L. Wang, E. J. Cairns and Y. Zhang. *Energy Environ. Sci.*, 2011, **4**, 5053-5059.
16 G. Zheng, Y. Yang, J. J. Cha, S. S. Hong and Y. Cui, *Nano Lett.*, 2011, **11**, 4462-4467.
17 J. Schuster, G. He, B. Mandlmeier, T. Yim, K. T. Lee, T. Bein and L. F. Nazar, *Angew. Chem. Int. Ed.*, 2012, **51**, 3591-3595.
18 S. Xin, L. Gu, N. H. Zhao, Y. X. Yin, L. J. Zhou, Y. G. Guo and L. J. Wan, *J. Am. Chem. Soc*., 2012, **134,** 18510-18513.
19 G. Zhou, L. C. Yin, D. W. Wang, L. Li, S. Pei, I. R. Gentle, F. Li and H. M. Cheng, *ACS Nano*, 2013, **7**, 5367-5375.
20 S. Lu, Y. Cheng, X. Wu and J. Liu, *Nano Lett.*, 2013, **13**, 2485-2489.
21 N. Li, M. Zheng, H. Lu, Z. Hu, C. Shen, X. Chang, G. Ji, J. Cao and Y. Shi, *Chem. Commun.*, 2012, **48**, 4106-4108.
22 M. Q. Zhao, X. F. Liu, Q. Zhang, G. L. Tian, J. Q. Huang, W. Zhu and F. Wei, *ACS Nano*, 2012, **6**, 10759-10769.
23 Y. Yang, G. Yu, J. J. Cha, H. Wu, M. Vosgueritchian, Y. Yao, Z. Bao and Y. Cui, *ACS Nano*, 2011, **5**, 9187-9193.
24 F. Wu, J. Chen, R. Chen, S. Wu, L. Li, S. Chen and T. J. Zhao, *J. Phys. Chem. C*, 2011, **115**, 6057-6063.
25 H. Chen, W. Dong, J. Ge, C. Wang, X. Wu, W. Lu and L. Chen, *Scientific Reports*, 2013, **3**, 1910.
26 L. Xiao, Y. Cao, J. Xiao, B. Schwenzer, M. H. Engelhard, L. V. Saraf, Z. Nie, G. J. Exarhos and J. Liu, *Adv. Mater.* 2012, **24**, 1176-1181.
27 Y. Zhang, Z. Bakenov, Y. Zhao, A. Konarov, T. N. L. Doan, M. Malik, T. Paron and P. Chen, *J. Power Sources*, 2012, **208**, 1-8.
28 Y. Fu and A. Manthiram, *J. Phys. Chem. C*, 2012, **116**, 8910-8915.
29 Y. Fu and A. Manthiram, *Chem. Mater.*, 2012, **24**, 3081-3087.
30 W. Zhou, Y. Yu, H. Chen, F. J. DiSalvo and H. D. Abruña, *J. Am. Chem. Soc.*, 2013, **135**, 16736-16743.
31 W. Li, Q. Zhang, G. Zheng, Z. W. She, H. Yao and Y. Cui, *Nano Lett.*, 2013, **13**, 5534-5540.
32 C. Zhou, Y. Zhang, Y. Li and J. Liu, *Nano Lett.*, 2013, **13**, 2078-2085.
33 H. Zhang, Q. Zhao, S. Zhou, N. Liu, X. Wang and F. Wang, *J. Power Sources*, 2011, **196**, 10484-10489.
34 D. B. Nash, *Appl. Optc.*, 1986, **25**, 2427-2433.